https://doi.org/10.5194/os-2021-5
Preprint. Discussion started: 5 February 2021
© Author(s) 2021. CC BY 4.0 License.

Ocean Science
Discussions
Open Access
EGU

On the Role of Westerly Wind Anomalies in the Development of the 1982-1983 El Niño

David J. Webb
National Oceanography Centre, Southampton SO14 3ZH, U.K.
Correspondence: D.J.Webb (djw@noc.ac.uk)

Abstract.

A recent study of two strong El Niños highlighted the potential importance of a region of low sea level that developed in the western equatorial Pacific prior to the El Niños of 1982-1983 and 1997-1998. Here the cause of the low sea level in 1982 is investigated using a series of runs of a global ocean model with different wind fields and initial conditions.

The results indicate that the low sea level was due to the increased wind shear that developed just north of the Equator during 1982. This generated Ekman divergence at the latitudes of the North Equatorial Trough, raising the underlying density surfaces and increasing the depth of the trough. This also increased the strength of the North Equatorial Counter Current which lies on the southern slope of the trough.

The anomalous westerly winds associated with Madden Julian Oscillations are often held responsible for triggering El Niños through the generation of westerly wind bursts and the resulting equatorial Kelvin waves in the ocean. However if Webb (2018) is correct, the present results imply that a different physical process was involved in which Ekman divergence due to the same winds, increased the heat transported by the North Equatorial Counter Current early in the year and ultimately caused the strong 1982-1983 El Niño.

Copyright statement. The works published in this journal are distributed under the Creative Commons Attribution 4.0 License. This licence does not affect the Crown copyright work, which is re-usable under the Open Government Licence (OGL). The Creative Commons Attribution 4.0 License and the OGL are interoperable and do not conflict with, reduce or limit each other.

1 Introduction

When Wyrtki (1973, 1974) studied tide gauge data from the equatorial Pacific, he found that the strong (or classic) El Niños were correlated with increased differences in sea level across the North Equatorial Counter Current (NECC). As such sea level differences are balanced by geostrophic currents, the increased difference implied that the NECC was stronger during an El Niño and so would carry more warm water than normal out of the western Pacific warm pool across to the eastern side of the ocean. He hypothesised that it was this increased transport which ultimately caused the large scale changes in atmospheric circulation.

https://doi.org/10.5194/os-2021-5
Preprint. Discussion started: 5 February 2021
© Author(s) 2021. CC BY 4.0 License.


For reasons that are not understood this hypothesis was not developed further, but recently Webb (2018), in an analysis of results from a high resolution run of the Nemo global ocean model, concluded that changes in sea level and changes the strength of the NECC in the western Pacific, near 6° N, were key precursors to the development of the strong El Niños of 1982-1983 and 1997-1998.

Webb (2018) identified other mechanisms that appeared to aid the development of the El Niño, but these only started operating once water from the west Pacific warm pool had started moving eastwards. Thus the lowering of sea level in western Pacific and the resulting increase in the strength of the NECC appeared to be critical factors.

1.1 Aims

Webb (2018) also found that the drop in sea level in the western Pacific coincided with the arrival of the annual Rossby wave at 6° N. Initially it appeared that the drop may be due to an increased amplitude of the Rossby wave in years when a strong El Niño developed, but further analysis has shown that in such years the wave was not unusually large when it crossed the central Pacific.

Another possible explanation is that the stratification in the Pacific, prior to an El Niño, is sufficient to focus the annual Rossby wave and so cause the region of lower than normal sea level. Alternatively the low sea level may not be connected with the annual Rossby wave and instead is due to some other process associated with the wind field. This could be a local feature occurring at or just before the period when sea level drops. Alternatively it could be a response to forcing elsewhere in the ocean which, like the Rossby waves, later propagates into the western Pacific.

To help clarify the cause of the drop in sea level, this paper reports on series of short ocean model runs, which focus the changes sea level prior to the 1982-1983 El Niño. The model used is a 1/4°global ocean model based on the original Occam model (de Cuevas et al., 1999). In each run, the model is initialised from one of the archive datasets from the original run of the Nemo model and forced with ocean surface stresses calculated during the same run.

1.2 Structure of the report

In the first part of the paper, section 2 describes the model being used and how the model fields and forcing were converted from the 1/12 degree Nemo run to the grid of the 1/4 degree model.

Section 3 then describes two tests carried out to validate the lower resolution model. In these the model was started from the Nemo archive datasets from early January 1981 and 1982 and then run for a year using the surface wind stresses from the same year. The resulting model fields were compared with the results from the original Nemo run.

The second part of the paper is concerned with a series of further runs of the Occam model with different wind fields. In this, section 4 reports on two runs where the model was again stated from early January 1981 and 1982, but with the wind forcing is from the opposite year. The results show that the main changes in sea level depend primarily the wind field and, to first order, are independent of the stratification at the start of the run.

In section 5, the test using the 1982 initial conditions with 1981 winds, is repeated but starting later in the year when the annual Rossby wave has developed and is starting to cross the central Pacific. This is done as a check to see if some property of

https://doi.org/10.5194/os-2021-5
Preprint. Discussion started: 5 February 2021
© Author(s) 2021. CC BY 4.0 License.


the Rossby wave is responsible for the sea level drop in the western Pacific. The results are similar to the earlier test, indicating that the wind generated Rossby wave is not responsible for the drop in sea level.

Section 6 takes the study further with a run designed to investigate whether the winds causing the drop in sea level are local to the western equatorial Pacific or propagate in from other parts of the ocean. The results show that it is the local winds that are responsible.

This leads to the final part of the paper where in Section 7, a study is made of the Ekman pumping in the western Equatorial Pacific due to the local winds. This concludes that the drop of sea level in the model runs is consistent with an enhanced level of Ekman suction that occurred north of the Equator during the first half of 1982.

The final section discusses these results and how they affect our understanding of how and why strong El Ninõs develop.

2 The Occam 1/4° global ocean model

The study reported here makes use of a recent version of the Occam global ocean model (Webb et al., 1997; de Cuevas et al., 1999). Occam is a primitive equation model, based on the Bryan-Cox-Semtner series of models (Bryan, 1969; Cox, 1989; Semtner, 1974).

It uses a regular latitude-longitude grid for all the oceans except the North Atlantic and Arctic. For the latter it uses a second rotated latitude-longitude grid which is matched to the first grid at the Equator. The Bering Strait between the Arctic and the North Pacific is modeled with a simple channel model.

This version of Occam has 1/4 degree resolution in both longitude and latitude. In the vertical it has 66 levels, instead of the 75 levels of the Nemo run, and makes use of an existing global topography has previously been checked against a database of critical oceanographic sills (Thompson, 1996). Both models use increased vertical resolution in the surface layers, Occam using 24 layers in the top 300m and Nemo 34 layers, the difference being primarily due to Nemo's extra resolution in the top 100m.

Occam uses harmonic mixing in the horizontal and the scheme of Pacanowski and Philander (1981) for vertical mixing. For horizontal advection it uses the second order split-quick scheme (Webb et al., 1998) for both momentum and tracers. For vertical advection it uses the scheme of Webb (1995).

Occam was chosen for these tests primarily because of its computational efficiency and because the amount of computer time available was limited. The efficiency arises partly because, unlike Nemo, it uses a regular grid and partly because the code includes fewer of the complex physical options included in Nemo.

However most ocean models are limited not by the speed of the processor but by the lengthy time needed to transfer data from main memory. Occam's main advantage is that it overcomes this by vectorising the code in the vertical[1].

[1]This means that all the variables needed to time step the cells in a vertical column are held in high speed cache at the same time and no extra references to main memory are required. Also when moving from one column of ocean cells to the next, most of the data required is already in cache.

https://doi.org/10.5194/os-2021-5
Preprint. Discussion started: 5 February 2021
© Author(s) 2021. CC BY 4.0 License.


2.1 Initialisation and forcing

The model runs reported here were initialised by averaging the archived data from the high-resolution Nemo model onto the Occam grid. Variable values within each Occam ocean cell were calculated by averaging over the intersection of the Occam and Nemo cells. In the case of vector quantities, vectors were rotated to the Occam grid before averaging.

The runs were also carried out with zero flux of heat and salt across the ocean surface. Each run is only for a few months and, although the surface temperatures and salinities are affected, this approximation allows the analysis to concentrate on the effects of the wind stress and of advection and diffusion within the ocean.

Each Nemo archive datasets contain the ocean and forcing fields averaged over the previous 5 days. Thus when initialising the Occam model and when specifying the wind forcing, the time of each Nemo dataset is set to the central time of the averaging period. However when specifying particular Nemo archive files, the original archive date is used.

The use of five day averages filters out all the high frequency components of the wind field and also means that the ocean state used to initialise the Occam model may be unusually smooth. The resulting lack of high frequency oscillations may affect vertical mixing in the ocean but should otherwise have little effect on lower frequency variations in sea level and current velocity, which are the focus of this study.

3 Validation

The use of the Occam 1/4 degree model for short runs was validated by comparing the model results over a full year with the results from the Nemo 1/12 degree run.

For the two cases reported here, the model was initialised from the Nemo archive datasets made on the 5th January 1981 and 1982. The run was then continued for a full year using the Nemo archived winds from that year.

3.1 Comparison of 1981 results

This paper is primarily concerned with the behaviour of sea level along 6° N in the Pacific. Fig. 1 compares the Occam model sea levels at this latitude with the 1981 sea levels of the full Nemo run.

The figure shows that the response of the two models is similar, both models showing short wavelength features due to tropical instability eddies and both showing a similar annual Rossby wave. This arrives in the western Pacific just after mid-year, but in both cases there is only a reasonably small drop in sea level in the far western Pacific.

Fig. 2 compares sea levels along the equator. Again there is reasonable agreement, both figures showing equatorial Kelvin waves of similar strength and both showing similar variations in sea level in the far west.

Figs. 4 to 7, compare the surface temperature and sea level fields from the two models around the 4th June and 2nd September 1981. In both sets of temperature figures, the Occam model tends to be warmer than Nemo in the southern hemisphere and cooler than Nemo in the north. This is to be expected as Occam lacks the surface heating in the northern summer and the cooling in the southern winter.

https://doi.org/10.5194/os-2021-5
Preprint. Discussion started: 5 February 2021
© Author(s) 2021. CC BY 4.0 License.


The sea level figures show better agreement. This is true for the large scale gyres of the north and south Pacific but, more importantly for this study, there is also good agreement in the development of the ridges and troughs on and just north of the Equator. Note, for example in the west equatorial Pacific, the height and extent of the maximum near the Equator and the depth and extent of the region of minimum sea level that develops just to the north-east of Mindinau.

3.2 Comparison of 1982 results

The following six figures provide a similar set of comparisons for the classic El Niño year of 1982. In this year both models show that, at 6° N, the drop in sea level in the western Pacific, associated with the arrival of the annual Rossby wave, is much stronger than in 1981 (a more normal year). Webb (2018) argued that it was this drop which generated the increase the NECC strength which triggered the development of a classic oceanographic El Niño.

Similarly in Fig 8, both models show the movement of high sea levels into the central Pacific during the second half of the year, which again increased the strength of the NECC.

Figs. 9 to 12, compare surface temperatures and sea level during 1982. Again the temperature plots show that the Occam is cooler in the northern hemisphere and warmer in the southern hemisphere.

The sea level plots show that in both models show a similar extension of the North Pacific Trough towards the west and a similar weakening of both the Equatorial Trough and the strength of tropical instability waves. On the Equator they also show a similar movement of the region of maximum sea level from the western Pacific to the central Pacific.

In conclusion, although the Occam model has only a third of the horizontal resolution of the Nemo model, and although it is missing surface fluxes of heat and fresh water, it is capturing the key differences in sea level between the normal year of 1981 and the El Niño year of 1982. On this basis it can be usefully used to study the development of the ocean El Niño in more detail.

4 Tests using wind stresses from different years

Although Webb (2018) identified a number of processes contributing to the development of a strong El Niño in 1982 and 1997, the study was not able to explain why the events started in those years and not, say, a year earlier or a year later.

One possibility, suggested by Webb (2018), is that there was something different about the stratification of the ocean in early 1982 and 1997, which focused the annual Rossby waves, so that they had a larger amplitude than usual once they reached the western Pacific. Another possibility is that the difference was due to the wind. This may have generated a stronger than normal annual Rossby wave that year. Alternatively some independent wind event may have occurred which lowered sea level in the western Pacific around the time that the annual Rossby wave arrived.

In an attempt to distinguish between these possibilities, the two Occam runs starting in January 1981 and 1982 were repeated, but this time forced by the winds from the opposite year. If focusing is important then then the January 1982 ocean forced by the 1981 winds, might generate a similar enhanced annual Rossby wave in the western Pacific. Alternative in the winds are important, then the January 1981 run, forced by the 1982 winds, would generate the low sea level in the western Pacific.

https://doi.org/10.5194/os-2021-5
Preprint. Discussion started: 5 February 2021
© Author(s) 2021. CC BY 4.0 License.

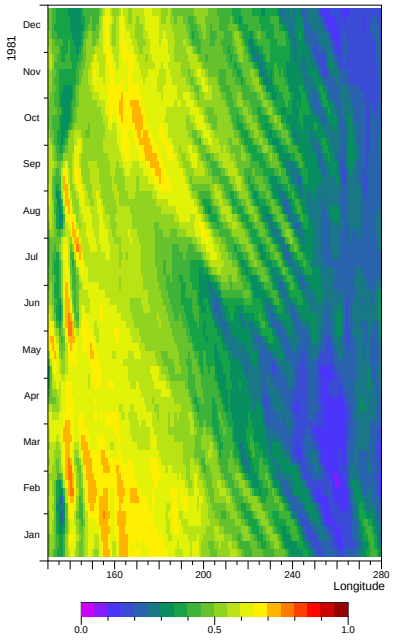

(a)

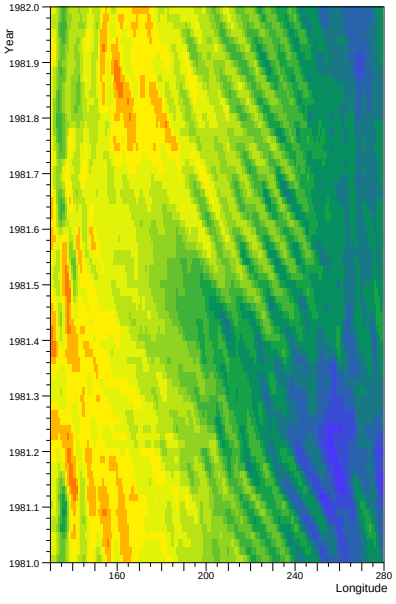

(b)

Figure 1. Hoffmuller diagram the sea level at 6° N in the Pacific for 1981, showing (a) sea level from the short Occam 1/4°model run and (b) from the Nemo 1/12°run. The figures are based on 1 °averages of the model data.

4.1 January 1982 ocean forced by 1981 winds

In this test, the model was initialised from the Nemo archive dataset dated the 5th January 1982, but then forced with winds from 1981. Figure 13 (top) shows how sea level developed at 6° N. Here the annual Rossby wave develops and propagates westwards as normal during the first few months of the year, but in mid-ocean the amplitude declines so by the time the wave reaches 180° E the signal is weak.

At the equator, sea level starts high in the western Pacific, as in the previous run with 1982 winds (Fig 8a), but as the year develops it stays in the west and there is no movement into the central Pacific.

Fig. 14 shows the surface temperature and sea level on the 4th June, a time when the transport by the NECC should start to increase. The temperature field is comparable with the run with 1982 winds (Fig 9) but the North Equatorial Trough is still only weakly developed and shows none of the westward extension expected for an El Niño year.

Fig. 15 is a similar plot from the autumn when the transport of warm water by the NECC would be large when an El Niño is developing. The temperature figure does show a narrow band of warm water advected by the NECC but the area of warm water is much weaker than was generated with the 1982 winds (Fig. 11). Sea level has a similar problem, the North Equatorial Trough being much shallower than that generated with 1982 winds.

https://doi.org/10.5194/os-2021-5
Preprint. Discussion started: 5 February 2021
© Author(s) 2021. CC BY 4.0 License.

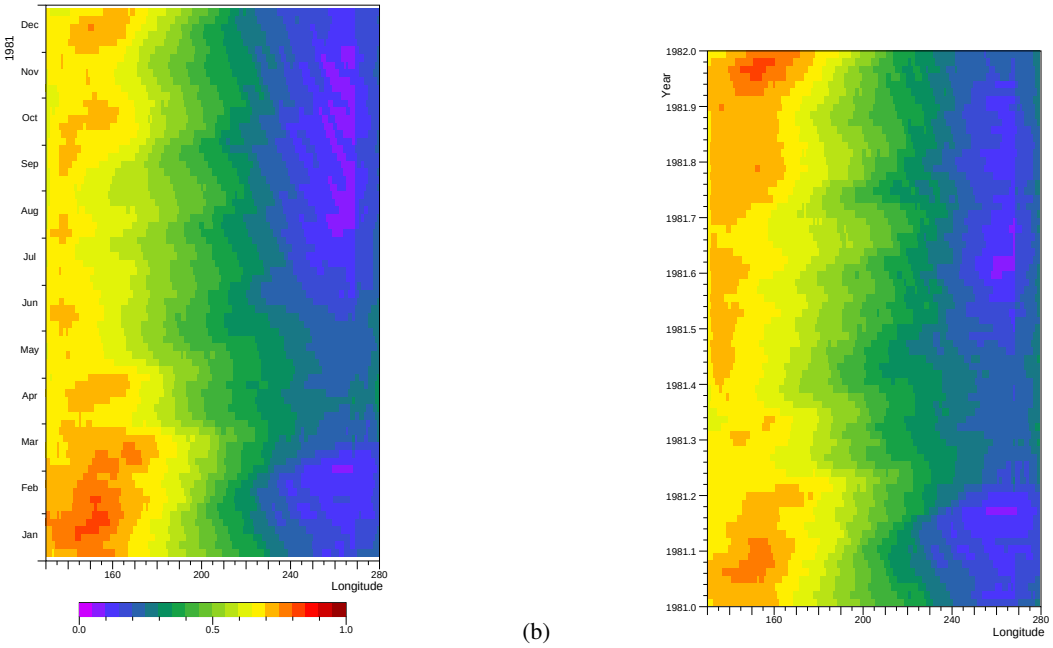

Figure 2. Hoffmuller diagram the sea level on the Equator in the Pacific for 1981, showing (a) sea level from the short Occam 1/4°model and (b) from the Nemo 1/12°run.

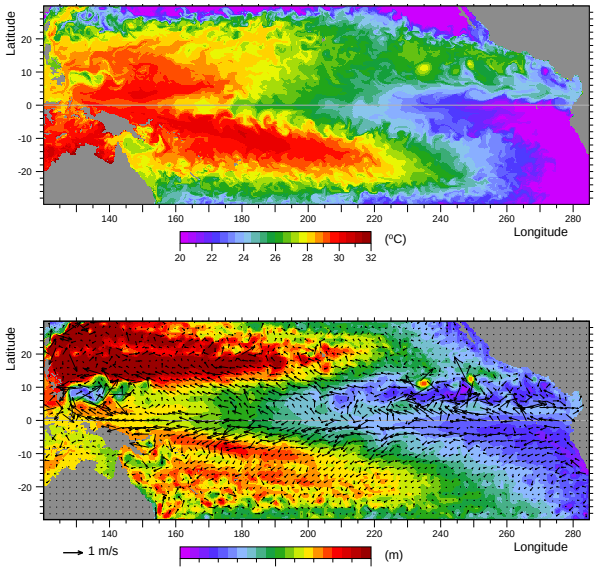

Figure 3. Plots of Occam model SST, SSH and surface velocities at the end of the 4th June 1981.

https://doi.org/10.5194/os-2021-5
Preprint. Discussion started: 5 February 2021
© Author(s) 2021. CC BY 4.0 License.

Ocean Science
Discussions
Open Access
EGU

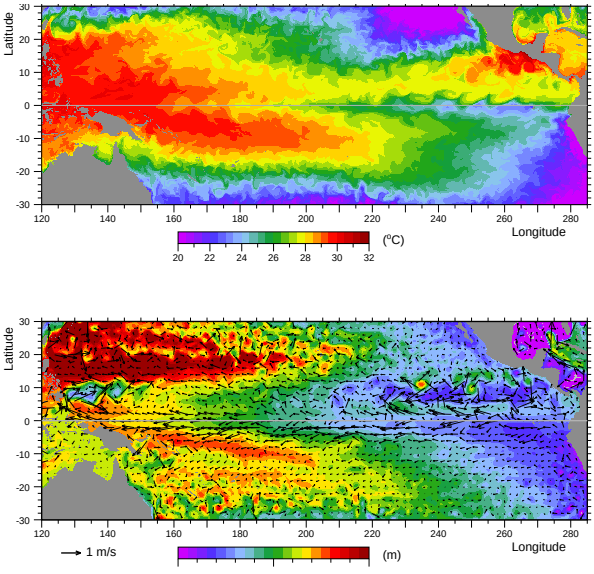

Figure 4. Plots of Nemo model SST, SSH and surface velocities from the average over the 5 days before the 4th June 1981.

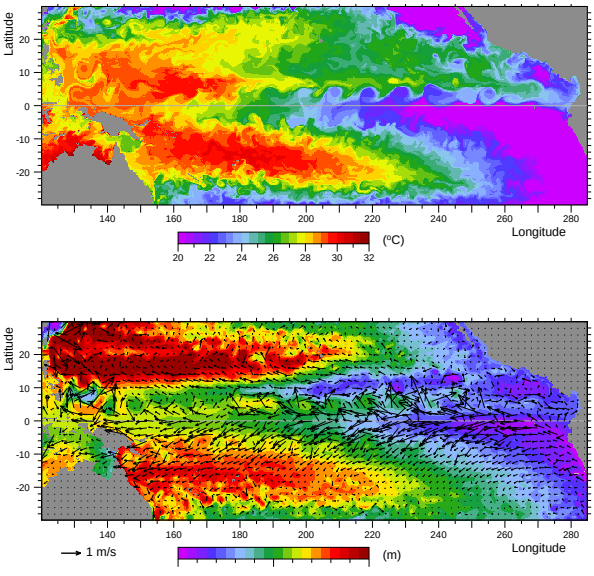

Figure 5. Plots of Occam model SST, SSH and surface velocities at the end of the 2nd September 1981.

After mid-year, changes in the wind system due to the developing El Niño will normally reduce the strength of the Equatorial Current and result in less energetic tropical instability eddies. Here because 1981 winds are being used, some of the differences seen in autumn are to be expected even if a stronger NECC had been triggered in mid-year.

https://doi.org/10.5194/os-2021-5
Preprint. Discussion started: 5 February 2021
© Author(s) 2021. CC BY 4.0 License.

Ocean Science
Discussions
Open Access
EGU

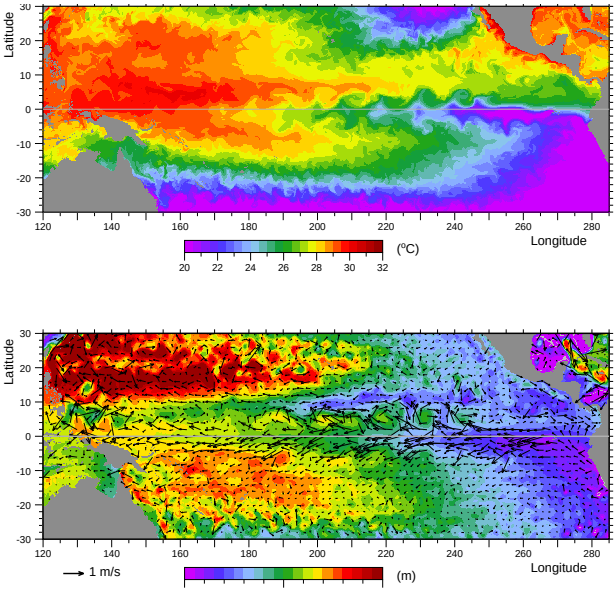

Figure 6. Plots of Nemo model SST, SSH and surface velocities from the average over the 5 days before the 2nd September 1981.

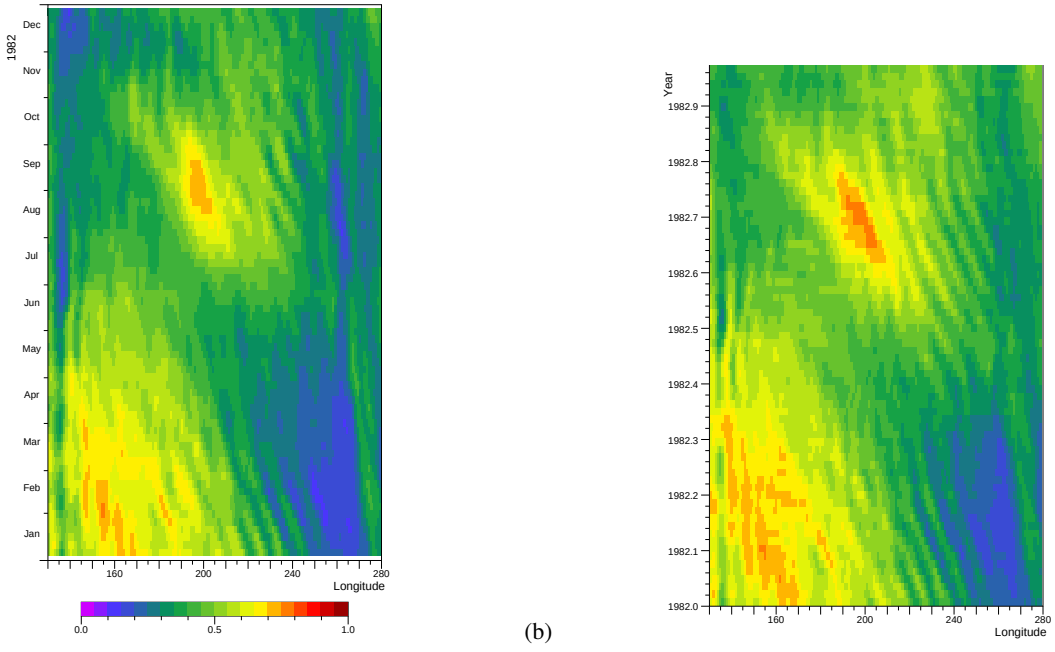

(a) (b)

Figure 7. Hoffmuller diagram the sea level at 6° N in the Pacific for 1982, showing (a) sea level from the Occam run and (b) from the Nemo run.

https://doi.org/10.5194/os-2021-5
Preprint. Discussion started: 5 February 2021
© Author(s) 2021. CC BY 4.0 License.

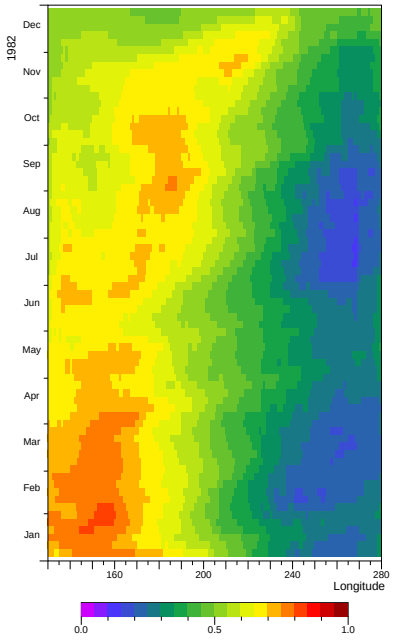

(a)

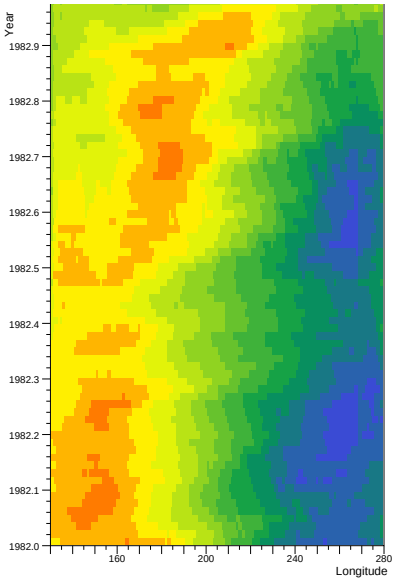

(b)

Figure 8. Hoffmuller diagram the sea level on the Equator in the Pacific for 1982, showing (a) sea level from the Occam run and (b) from the Nemo run.

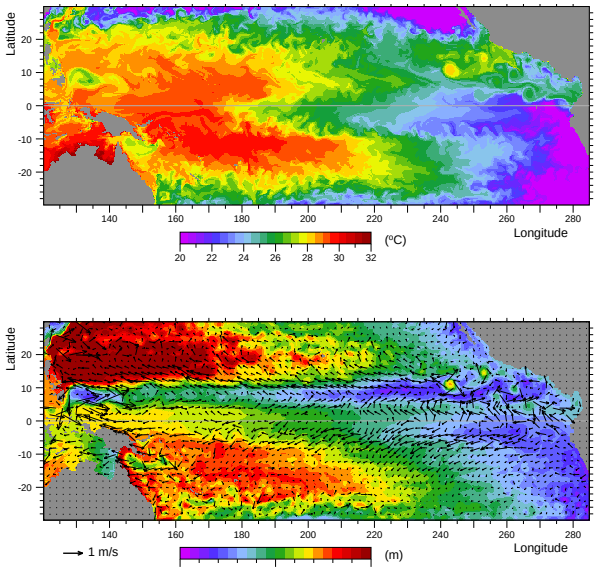

Figure 9. Plots of Occam model SST, SSH and surface velocities at the end of the 4th June 1982.

https://doi.org/10.5194/os-2021-5
Preprint. Discussion started: 5 February 2021
© Author(s) 2021. CC BY 4.0 License.

Ocean Science
Discussions
Open Access
EGU

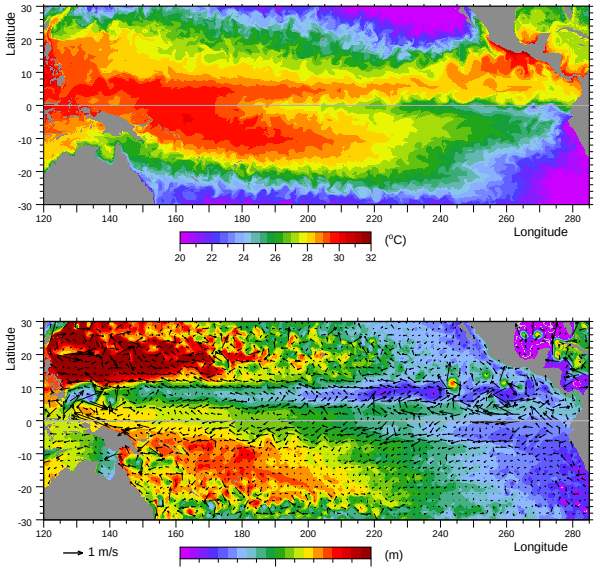

Figure 10. Plots of Nemo model SST, SSH and surface velocities from the average over the 5 days before the 4th June 1982.

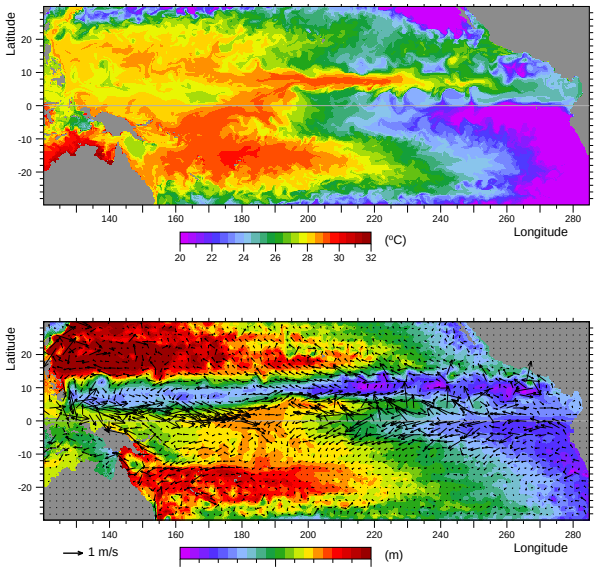

Figure 11. Plots of Occam model SST, SSH and surface velocities at the end of the 2nd September 1982.

The main conclusion from this run is that the ocean state at the start of 1982 was not sufficient to trigger an El Nino in mid-year. Although a reasonable annual Rossby wave was generated early in the year (Fig 13), this was not focused and did not generate or contribute to the lowering of sea level in the western Pacific.

https://doi.org/10.5194/os-2021-5
Preprint. Discussion started: 5 February 2021
© Author(s) 2021. CC BY 4.0 License.

Ocean Science
Discussions
Open Access
EGU

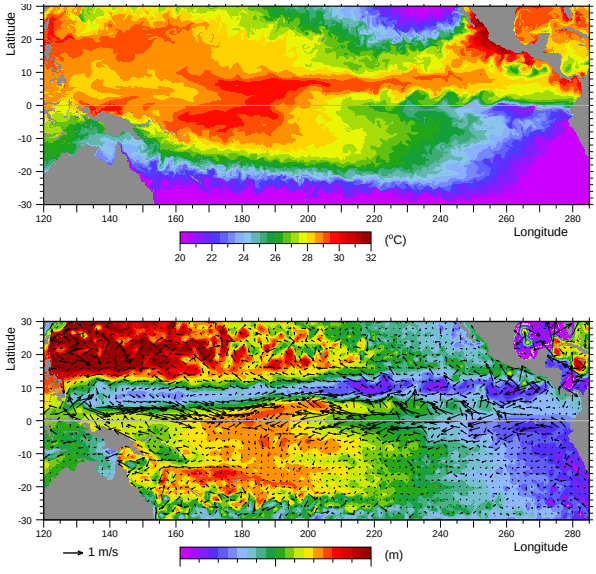

Figure 12. Plots of Nemo model SST, SSH and surface velocities from the average over the 5 days before the 2nd September 1982.

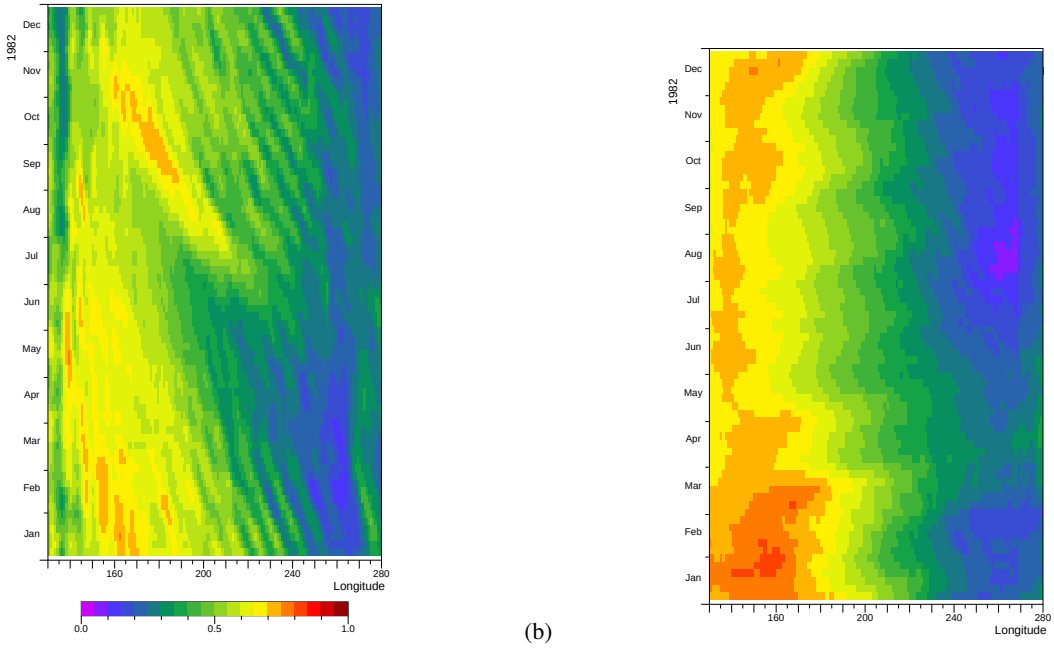

Figure 13. Hoffmuller diagram the sea level from the Occam model during 1982, when started from Nemo model archive for the 5th January 1982 but forced by 1981 winds for (above) 6° N and (below) at the Equator.

https://doi.org/10.5194/os-2021-5
Preprint. Discussion started: 5 February 2021
© Author(s) 2021. CC BY 4.0 License.

Ocean Science
Discussions
Open Access
EGU

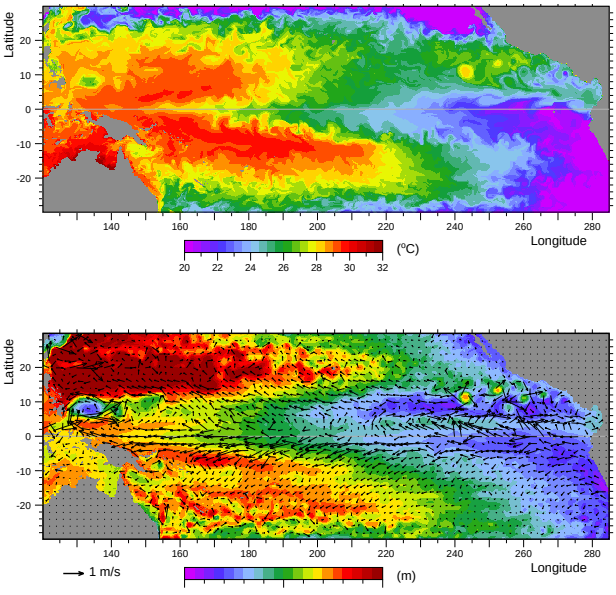

Figure 14. Plots of Occam model (top) SST, (bottom) SSH and surface velocities, at the end of the 4th June 1982, in the run started from the Nemo archive of the 5th January 1982 but forced with 1981 winds.

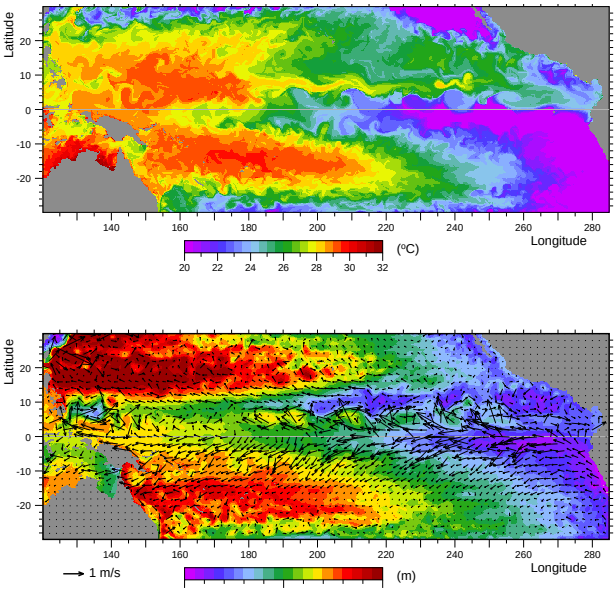

Figure 15. Plots of Occam model SST, SSH and surface velocities at the end of the 2nd September 1982, of the run started from the Nemo archive of the 5th January 1982 but forced with 1981 winds.

https://doi.org/10.5194/os-2021-5
Preprint. Discussion started: 5 February 2021
© Author(s) 2021. CC BY 4.0 License.

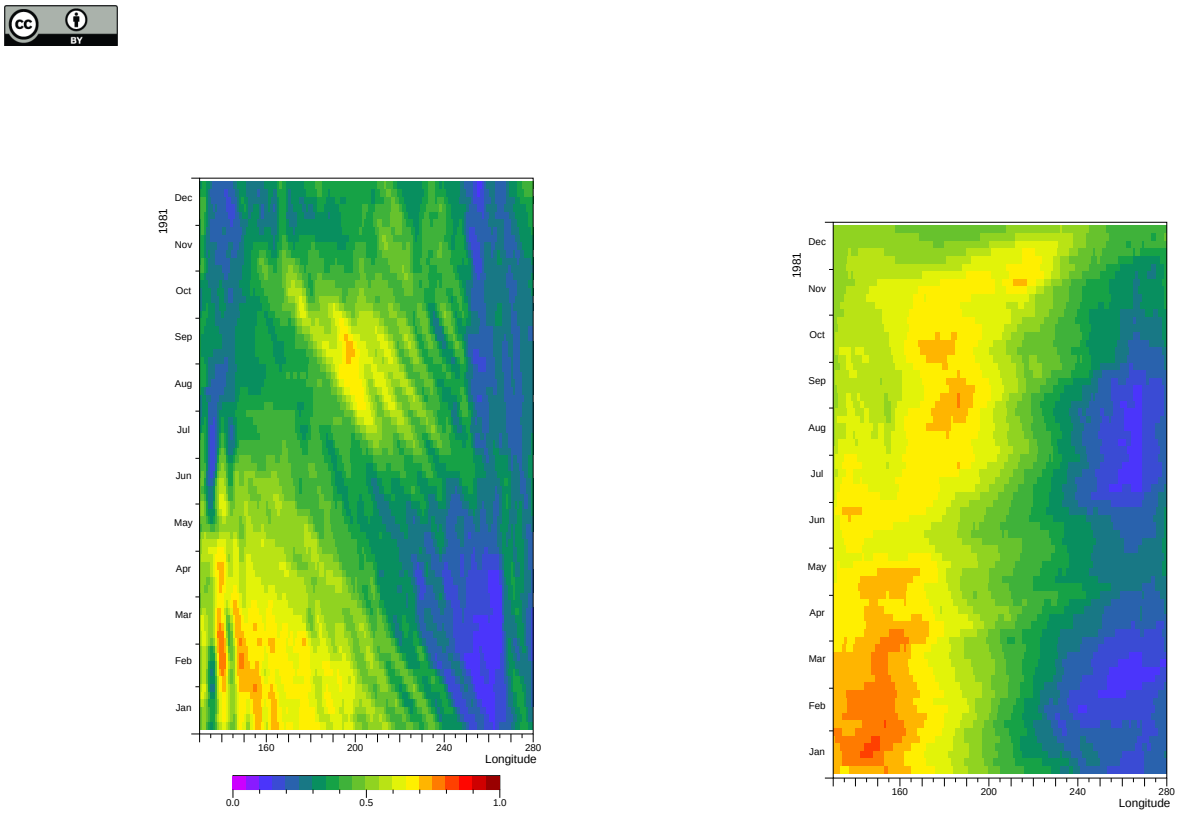

Figure 16. Hoffmuller diagram the sea level from the Occam model during 1981, when started from the Nemo model archive from the 5th January 1981 but forced by 1982 winds for (above) 6° N and (below) at the Equator. [Review version: Left and right when single column]

4.2 January 1981 ocean forced by 1982 winds

In the second test, the ocean is initialised from the Nemo archived dataset dated the 5th January 1981, but then forced with 1982 winds. Figure 16 (top) shows the sea level during the year at 6° N. The annual Rossby starts as before, but this time it continues past 180° E and links up with a region of low sea level in the western Pacific - as might be expected in an El Niño year.

On the Equator, Fig. 16 (bottom), the ocean again starts with high sea levels in the west. In mid-year these move into the central Pacific - again as might be expected in an El Niño year.

Figure 17 shows that in mid-year the distribution of sea surface temperature is similar to the other Occam runs, but sea level shows a well developed North Equatorial Trough with a strong NECC developing on its southern slope.

By September (Fig. 18), the trough has developed further and the temperature plot shows warm surface water being advected rapidly into the eastern Pacific. The area of warm water involved is not as large as in the original Nemo run, but as with Fig. 11, this is probably a result of setting the surface flux of heat to zero in these test runs.

One conclusion from this test is that the ocean will produce an El Niño like response when forced by the winds from an El Niño year. This has been reported before, but based on the large sea level and temperature anomalies that develop in the western Pacific cold pool towards the end of the first year of a classic oceanographic El Niño.

https://doi.org/10.5194/os-2021-5
Preprint. Discussion started: 5 February 2021
© Author(s) 2021. CC BY 4.0 License.

Ocean Science
Discussions
Open Access
EGU

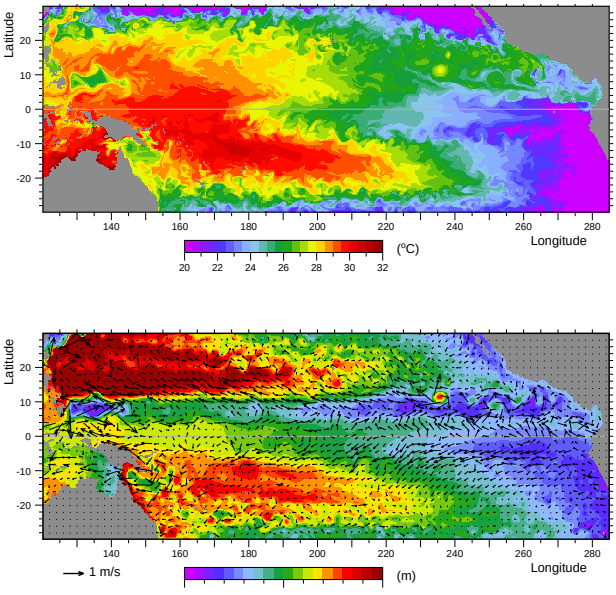

Figure 17. Plots of Occam model SST, SSH and surface velocities at the end of the 4th June 1981, of run started from Nemo model on 5th January 1981 but forced with 1982 winds.

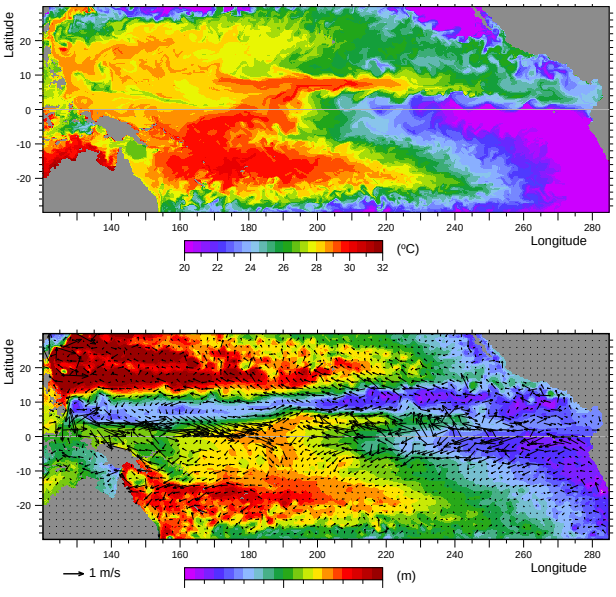

Figure 18. Plots of Occam model SST, SSH and surface velocities at the end of the 2nd September 1981, of run started from Nemo model on 5th January 1981 but forced with 1982 winds.

https://doi.org/10.5194/os-2021-5
Preprint. Discussion started: 5 February 2021
© Author(s) 2021. CC BY 4.0 License.

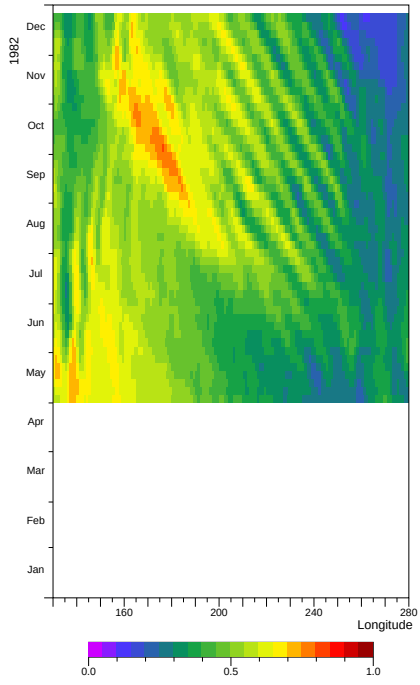

Figure 19. Hoffmuller diagram for the sea level at 6° N during 1982, when started from the Nemo model archive from the 30th April 1982 but forced by 1981 winds.

The cold pool is the region of cold water lying near the equator in the western Pacific which oceanographers associate with the upwelling of cold undercurrent water. During an El Niño, the easterly winds and undercurrent become weaker, less cold water is upwelled and as a result sea surface temperatures increase. This reduces reduces the density of sea water, so sea level also rises.

The present case is different in that it shows the winds having a significant effect during the first half of the year, well before any changes in the atmospheric convection regime are noticeable. What is not clear is whether, during this period, the increased depth of the North Equatorial Trough is due to a change in the mean winds during the period or due to one or more isolated events.

It is also not clear whether it is a local change in the winds along the line of the Trough, or whether the key wind forcing occurs elsewhere and the signal propagates into the region lowering the level of the Trough. The remaining tests reported here are an attempt to obtain a clearer answer to these questions.

5 Tests starting in late April

One possibility that has not been discounted is that winds early in the 1982 generated a Rossby wave, or similar, which was later responsible for the drop sea level drop in the western Pacific. To test this hypothesis, the model was started from from

https://doi.org/10.5194/os-2021-5
Preprint. Discussion started: 5 February 2021
© Author(s) 2021. CC BY 4.0 License.

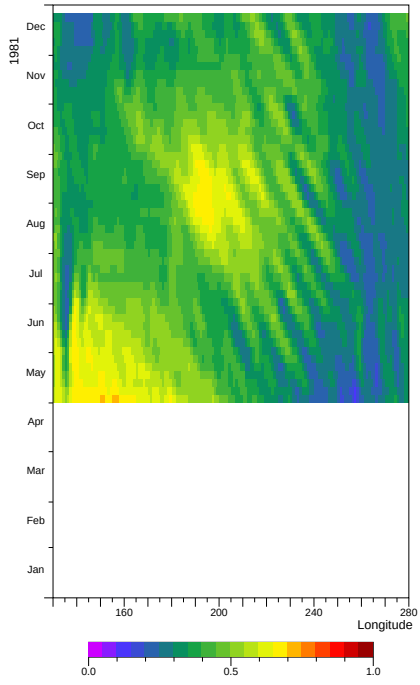

Figure 20. Hoffmuller diagram for the sea level at 6° N during 1981, when started from the Nemo model archive from the 30th April 1981 but forced by 1982 winds,

the Nemo archive dataset dated the 30th April 1982 and then forced with the 1981 winds. The start date is just before the start of the drop in sea level in the western Pacific. If the Rossby or other waves are responsible, then by that date they should be established enough to reproduce the drop in sea level despite the change in the wind field.

The result at 6° N is shown in Fig. 19. It shows that under these conditions there is no significant drop in sea level. Thus, although the test does not exclude events occurring before the 30th April having some impact, they can not be the prime cause of the sea level drop.

The complimentary test was also carried out, in which the ocean was started from the 30th April 1981 but forced with 1982 winds. The result, shown in Fig. 20, shows that sea level does drop. This implies that it is the winds after the 30th April 1982 that are responsible.

6 A Further Test with the Winds

Figure 21 shows the difference between the 1982 and 1981 wind stress vectors for the Pacific when averaged between the 16th March and the 8th August. It shows that in the western Pacific near the Equator, there is a significant westerly component to the wind stress anomaly. North of New Guinea this drops to zero near 10° N. This distance is typical of the atmospheric equatorial

https://doi.org/10.5194/os-2021-5
Preprint. Discussion started: 5 February 2021
© Author(s) 2021. CC BY 4.0 License.

Ocean Science
Discussions
Open Access
EGU

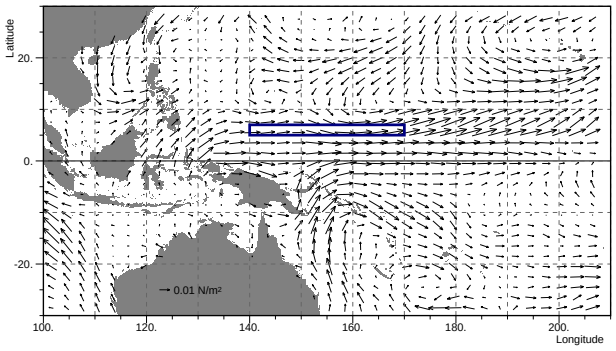

Figure 21. Wind stress vector anomaly, for the period 16th March to the 8th August 1982 relative to the same period in 1981. The blue rectangle shows the region between 140° E and 170° E and between 5° N and 7° N.

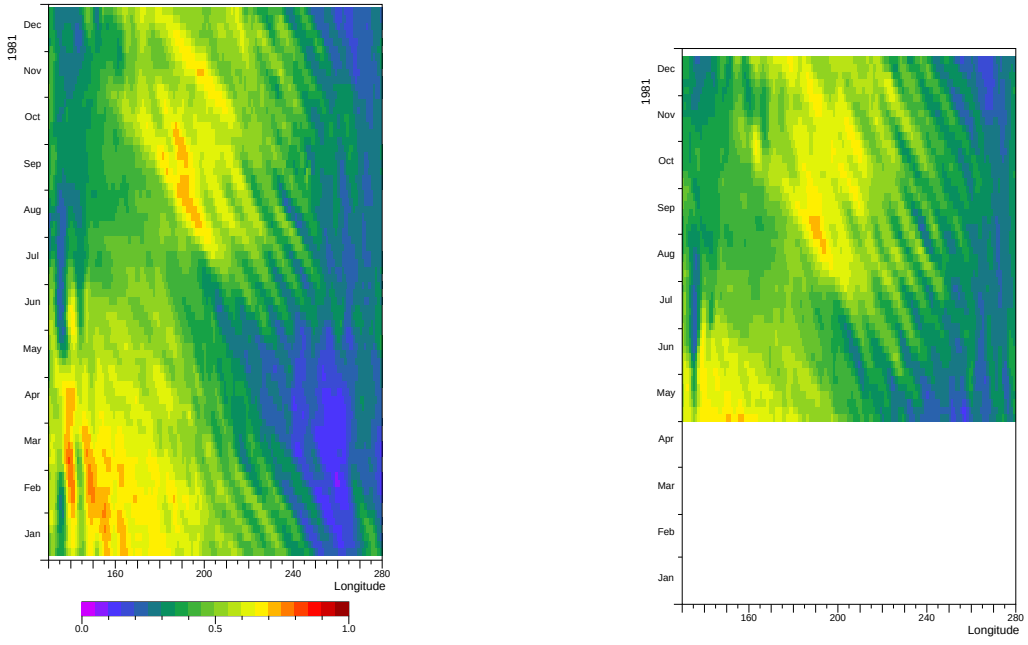

Figure 22. Hoffmuller diagram for the sea level at 6° N during 1981, forced by the combination of 1981 and 1982 winds described in the main text when started from the NEMO archive for (above) 5th January 1981, (below) 30th April 1981. [Review version: Left and right.]

Rossby radius, a scale which also determines the northward extent of Madden-Julian Oscillations (MJOs). Thus the anomaly and the large north-south gradient in the wind stress may be a result of MJOs.

Further east the ITCZ often lies close to 10° N. It is not clear whether this is also related to the equatorial Rossby radius, but the figure shows that this is also an region where both the wind stress anomaly and its north-south gradient in the can be large.

https://doi.org/10.5194/os-2021-5
Preprint. Discussion started: 5 February 2021
© Author(s) 2021. CC BY 4.0 License.

Ocean Science
Discussions
Open Access
EGU

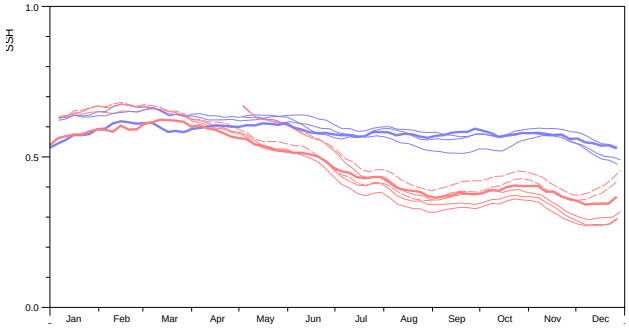

Figure 23. Sea level in the different runs averaged between 140° E and 170° E and between 5° N and 7° N. Red lines correspond to runs forced by 1982 winds, blue to 1981 winds. Thick lines are from the original Nemo run, thin lines are from the occam runs. The dashed lines corresponds to the runs started in 1981 but with 1982 winds only in the western Pacific.

To see if the local wind fields in the western Pacific were responsible for the drop in sea level in 1982, a modified wind field was constructed which combined both the 1981 and 1982 winds. The weighting for the 1982 winds was defined so that it equaled one within the region between 140° E to 180° E and the Equator and 15° N and was zero outside the region 130° E to 190° W and 10° S to 25° N. Linear interpolation was used between the two boundaries. Weighting for the 1981 field was set to one minus the 1982 weighting.

This results in the 1982 wind field being used for the area where the main sea level drop is observed and the 1981 wind fields being used elsewhere but with a smooth transition zone. The combined wind field was then used for two runs. As with the previous tests using 1982 winds, the first started from the ocean state for the 3rd January 1981 and the second from the 30th April 1981. If the drop in sea level is due to local winds then the change in sea level should be similar to those obtained using only the 1982 wind field.

The resulting sea levels along 6° N are shown in Fig. 22. In both cases sea level starts dropping in the western Pacific in early May, confirming the importance of the local winds.

6.1 Intercomparison

Fig. 23 shows the changes in sea level from the different runs, averaged over the region 140° E to 170° E and 5° N to 7° N, as outlined in fig. 21. The occam runs start with a slight offset from the corresponding runs of the Nemo model, due to the initial adjustment to the new coast and topography.

In this figure, colour is used to distinguish the different winds forcing the ocean, red for 1982 and blue for 1981. Even with the different starting conditions, the runs soon split into two distinct groups, sea levels with the 1981 winds staying roughly constant whereas the 1982 winds generate a 20 cm drop between March and August. As pressures in the deep ocean remain roughly constant, this drop in sea level must correspond to a significant rise in the density surfaces within the ocean.

https://doi.org/10.5194/os-2021-5
Preprint. Discussion started: 5 February 2021
© Author(s) 2021. CC BY 4.0 License.

Ocean Science
Discussions
Open Access
EGU

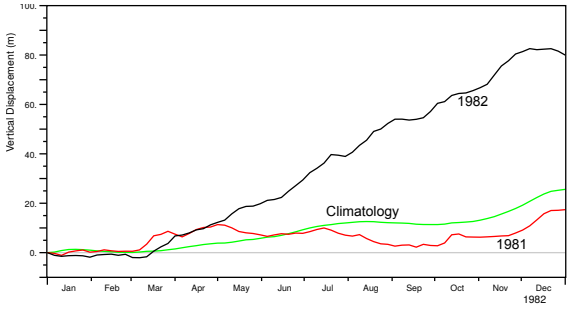

Figure 24. Integral over time of the vertical velocity due to Ekman divergence in the region bounded by 140° E, 170° E, 5° N and 7° N, during (black) 1982, (red) 1981, (green) climatology 1958-2015.

7 Winds and Ekman Divergence

Given that local winds appear to be responsible, the most likely cause of the rise in the density surfaces is that it is due to a divergence in the wind generated Ekman transport in the surface layers of the ocean.

Here the possibility is investigated by calculating the Ekman pumping in the region 140° E to 170° E and 5° N to 7° N.

If the Ekman transport vector is $E(\theta,\phi)$, where θ and ϕ are latitude and longitude, then

$$E(\theta,\phi) \quad = \quad \tau(\theta,\phi) \times \hat{n}/(\rho f(\theta)) \tag{1}$$

where $\tau(\theta,\phi)$ is the wind stress vector, $\hat{\boldsymbol{n}}$ the unit vertical vector, ρ is the density and $f(\theta)$ is the Coriolis term, equal to,

$$f(\theta) \quad = \quad 2\,\Omega\,\sin(\theta). \tag{2}$$

Ω is the angular rotation rate of the Earth.

The averaged vertical velocity in a region, due the divergence of the Ekman flux, is then given by integrating the outward flowing Ekman transport around the region of interest,

$$P \quad = \quad -(1/A) \oint E(\theta;\phi) \wedge \hat{n} \cdot d\hat{s}, \tag{3}$$

$$\quad = \quad (1/A) \oint \tau(\theta,\phi) \cdot d\hat{s}/(\rho f(\theta)). \tag{4}$$

where $\hat{\boldsymbol{s}}$ is the unit vector tangential to the boundary and A the area enclosed.

Fig. 24, shows the results obtained by integrating the vertical velocity over time. It shows that in 1982 the Ekman divergence was positive for most of the period between April and late November, and that it had the potential for raising density surfaces within the ocean by 80 m. During the period mid-March to mid-August the potential rise is approximately 50 m.

A noticeable feature of figs. 23 and 24 is that, during 1982, the drop in sea level and the vertical displacement due to the Ekman divergence are both relatively steady processes occuring over many months. There are short periods when the rate of change is reduced or reverses, but overall the results imply that the changes are a result of a long term systematic change in the wind field.

https://doi.org/10.5194/os-2021-5
Preprint. Discussion started: 5 February 2021
© Author(s) 2021. CC BY 4.0 License.

Ocean Science
Discussions
Open Access
EGU

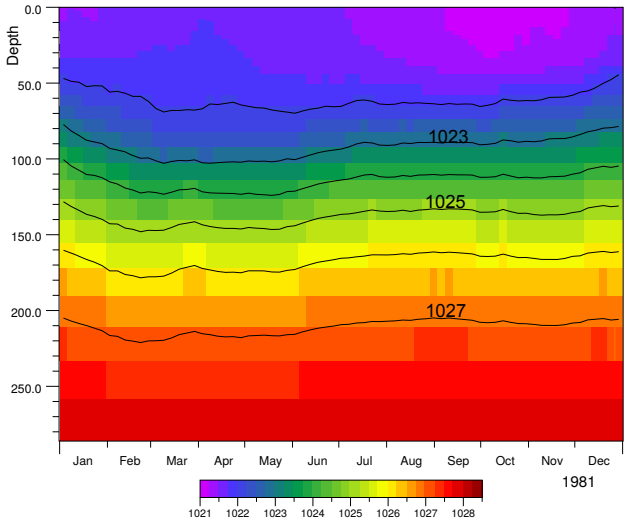

Figure 25. Nemo 1/12° model potential density during 1981, averaged between 140° E and 170° E and between 5° N and 7° N. Contours, interpolated from model layer values, at integer values of density ($\mathrm{kg/m^3}$).

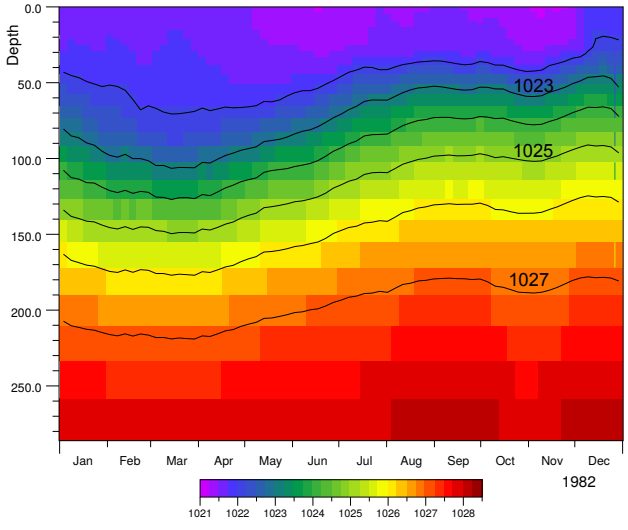

Figure 26. Nemo 1/12° model potential density during 1982, averaged between 140° E and 170° E and between 5° N and 7° N. Contours at integer values of density ($\mathrm{kg/m^3}$).

To check that the Ekman pumping is sufficient to cause the observed change in sea level, figs. 25 and 26 show the density profiles from the original Nemo 1/12° model run averaged over the same area as before.

https://doi.org/10.5194/os-2021-5
Preprint. Discussion started: 5 February 2021
© Author(s) 2021. CC BY 4.0 License.


Figure 25 shows that during 1981, the changes in the depth of the density surfaces were small and at most depths had balanced out by the end of the year.

In contrast, during 1982 (fig. 26), there was a significant shallowing of the density surfaces. The figure shows that in mid-March, water with densities of 1025 $\mathrm{kg\,m^{-3}}$ (approx 21.5° C) lay near 150 m, and that by mid-August it had risen to near 100 m. This rise of approximately 50 m is comparable with the Ekman pumping estimate. However after this period, although the negative Ekman pumping continued there was no further shallowing in the density surfaces near the surface and there is evidence of a rebound at depth.

The main conclusion to be taken from these results is that between mid-March and mid-August at the start of the 1982-1983 El Niño, there was a strong amount of negative Ekman pumping (i.e. Ekman suction) in the western Pacific around 6° N due to a wind anomaly. The results also indicate that this was due to a systematic change in the local wind field which lasted for many months.

Previously, the papers by Zhao et al. (2013) and Tan and Zhou (2018) both showed strong correlations between Ekman pumping north of the Equator and the behaviour of the NECC. However the present results emphasise how the changed NECC can then be an active trigger of strong El Niños rather than always representing a passive response to events elsewhere.

8 Conclusions

The primary aim of this study has been to understand the causes of the low sea levels that developed in the western Pacific along the line of the North Equatorial Trough early in the development of the strong 1982-1983 El Niño.

A comparison of results from the Nemo 1/12 degree and Occam 1/4 degree global ocean models indicated that that the latter was suitable for studying the development of the 1982-1983 El Niño in the Pacific.

The Occam model was then used in a series of short runs to determine which part of the wind field was responsible for the low sea levels. The tests in which the model was started from the ocean state at the beginning of 1981 and 1982 and forced by the winds from the opposite year, showed that the initial state of the ocean was not critical, but that the model needed the 1982 winds in order to generate the sea level drop in the western pacific.

Similar tests, starting in mid-April were used to check if Rossby or other waves, generated early each year were important. However the conclusion was that they had no significant effect.

In the final set of tests, the model was forced by 1981 winds everywhere except for a localised region in the western equatorial Pacific. In both cases these runs of the model reproduced the drop in sea level, indicating that it was primarily the local winds, acting around the same time as the drop in sea level, that were responsible.

A plot of the wind stress anomalies in 1982, showed that at latitudes between 5° N and 12° N in the western equatorial Pacific there can be a significant gradient in the wind stress. Because of this, the amount of Ekman pumping was calculated. It was found that in 1981 the term was small, but that in 1982 significant Ekman pumping occurred between April and November. The original Nemo model archive showed that from April onwards there was corresponding rise in the density surfaces, but that the rise stopped in August as the shallowest density surfaces neared the surface.

https://doi.org/10.5194/os-2021-5
Preprint. Discussion started: 5 February 2021
© Author(s) 2021. CC BY 4.0 License.


Allowing for this, the results indicate that the deepening of the North Equatorial Trough, between 130° E and 170° E during the early development of the 1982-1983 El Niño, was due to Ekman suction caused by a period of anomalous surface wind stress.

North of New Guinea the anomalous wind stress has a structure similar to that expected from the westerly wind phase of a Madden Julian Oscillation, with a maximum near the Equator and dropping to near zero at a latitude corresponding to the atmospheric Rossby radius. Further east the anomaly appears to be more connected to the shears associated with an active intertropical convergence zone.

El Niños are often thought to be triggered by Madden Julian Oscillations. Although not checked here it is possible that in 1982 one or more MJOs were initially responsible for the westerlies that developed north of New Guinea. The westerlies generated an eastward flowing current along the Equator which would have started moving the region of deep convection eastwards. There were also westerly wind bursts which generated equatorial Kelvin waves.

However acting over a period of months, the westerlies also increased the depth of the North Equatorial Trough through Ekman pumping. This increased the strength of the NECC, which then carried more warm water eastwards than was normal. Further east strong wind shears developed, associated with the ITCZ, again with the potential of deepening the North Equatorial Trough and increasing the strength of the NECC.

So in conclusion, a study of current and sea level changes in the Equatorial Ocean has emphasised the role of the wind shears north of the Equator and the large amount of Ekman divergence that results.

In the western equatorial Pacific this increased the depth of the North Equatorial Trough and increased the transport of the North Equatorial Counter Current. As discussed in Webb (2018) this was timed to connect with the increased transport due to the annual Rossby wave and so caused the strong El Niño of 1982-1983.

At a more general level, this study has also emphasised the mismatch between the ocean's equatorial Rossby radius, the scale of the ocean's tropical cell and the much large scale of the atmosphere's equatorial Rossby radius. Without this mismatch the North Equatorial Tough would probably not be so deep and the NECC would not have had such a important role in the development of the 1982-1983 El Niño.

Code and data availability. At the time of publication the Nemo model datasets are freely available at "http://gws-access.ceda.ac.uk/public/nemo/runs/ORCA0083-N06/means/". The Nemo ocean model code and its documentation are available from "http://forge.ipsl.jussieu.fr/nemo/wiki/Users". The occam model is based on the moma ocean model available from "https://github.com/djwebb/moma".

Author contributions. The author is responsible both the model runs and the analysis.

https://doi.org/10.5194/os-2021-5
Preprint. Discussion started: 5 February 2021
© Author(s) 2021. CC BY 4.0 License.

Acknowledgements. This work contributed to and was aided by the research programme of the Marine Systems Modelling group at the UK National Oceanography Centre, part of the Natural Environment Research Council. The Natural Environment Research Council helped fund the investigation through the NOC National Capability funding. Part of the analysis was carried out using the JASMIN Service at the UK Centre for Environmental Data Analysis, also funded by NERC.

https://doi.org/10.5194/os-2021-5
Preprint. Discussion started: 5 February 2021
© Author(s) 2021. CC BY 4.0 License.


References

Bryan, K.: A numerical method for the study of the circulation of the world ocean, Journal of Computational Physics, 4, 1255–1273, 1969.

Cox, M.: A primitive equation 3-dimensional model of the ocean, Ocean Group Technical Report 1, Geophysical Fluid Dynamics Laboratory, Princeton University, Princeton, N.J. 08542, 1989.

de Cuevas, B., Webb, D., Coward, A., Richmond, C., and Rourke, E.: The UK Ocean Circulation and Climate Advanced Modelling Project (OCCAM), in: High Performance Computing, edited by Allan, R., Guest, M., Simpson, A., Henty, D., and Nicole, D., pp. 325–336, Kluwer Academic, New York, 681 pp., 1999.

Pacanowski, R. and Philander, S.: Parameterization of vertical mixing in numerical models of tropical oceans, Journal of Physical Oceanography, 11, 1443–1451, 1981.

Semtner, A.: A general circulation model for the World Ocean, Technical Report No. 9, Department of Meteorology, University of California, Los Angeles, 1974.

Tan, S. and Zhou, H.: The observed impacts of the two types of El Niño on the North Equatorial Countercurrent in the Pacific Ocean, Geophysical Research Letters, 45, 10,439–10,500, https://doi.org/10.1029/2018GL079273, 2018.

Thompson, S. D.: Sills of the Global Ocean: a compilation, https://www.nodc.noaa.gov/woce/woce_v3/wocedata_2/bathymetry/sills/index.htm, 1996.

Webb, D.: The vertical advection of momentum in Bryan-Cox-Semtner ocean general circulation models, Journal of Physical Oceanography, 25, 3186–3195, 1995.

Webb, D., Coward, A., de Cuevas, B., and Gwilliam, C.: A Multiprocessor Ocean General Circulation Model Using Message Passing, Journal of Atmospheric and Oceanic Technology, 14 (1), 175–183, 10.1175/1520-0426(1997)014<0175:AMOGCM>2.0.CO;2, 1997.

Webb, D., de Cuevas, B., and Richmond, C.: Improved advection schemes for ocean models, Journal of Atmospheric and Oceanic Technology, 15, 1171–1187, 1998.

Webb, D. J.: On the role of the North Equatorial Current during a strong El Niño, Ocean Science, 14, 633–660, https://doi.org/10.5195/os-14-633-2018, 2018.

Wyrtki, K.: Teleconnections in the Equatorial Pacific Ocean, Science, 180(4081), 66–68, 1973.

Wyrtki, K.: Equatorial Currents in the Pacific 1950 to 1970 and Their Relation to the Trade Winds, Journal of Physical Oceanography, 4, 372–380, 1974.

Zhao, J., Li, Y., and Wang, F.: Dynamical response of the west Pacific North Equatorial Countercurrent (NECC) system to El Niño events, J. Geophys. Res. Oceans, 118, 2828–2844, https://doi.org/10.1002/jgrc.20196, 2013.